doi:10.3772/j.issn.1006-6748.2018.02.008

# The torsion model of soft tissue in virtual surgery①

Zhang Xiaorui(张小瑞)②[*,**], Wang Pengpai[*], Wei Sun[**], Liu jia[**], Zhu Lifeng[***]
([*]Jiangsu Engineering Center of Network Monitoring, Nanjing University of Information Science & Technology, Nanjing 210044, P. R. China)
([**]Jiangsu Collaborative Innovation Center of Atmospheric Environment and Equipment Technology (CICAEET), Nanjing University of Information Science & Technology, Nanjing 210044, P. R. China)
([***]School of Instrument Science and Engineering, Southeast University, Nanjing 210096, P. R. China)

**Abstract**

In order to solve the problem of real-time soft tissue torsion simulation in virtual surgeries, a torsion model based on coil spring is proposed to actualize real-time interactions and applications in virtual surgeries. The proposed model is composed of several connected coil springs in series. The sum of torsion deformation on every coil is equivalent to the soft tissue surface deformation. The calculation of the model is simple because the method for calculating the torsion deformation for each coil spring is the same. The virtual surgery simulation system is established on PHANTOM OMNI haptic device based on the OpenGL 3D graphic interface and VC ++ software, and it is used to simulate the torsion deformation of virtual legs and arms. Experimental results show that the proposed model can effectively simulate the torsion deformation of soft tissue while being of real-time performance and simplicity, which can well meet requirements of virtual operation simulations.

**Key words**: virtual surgery, soft tissue torsion, system simulation, coil spring model

## 0 Introduction

Nowadays, aging population in China keeps increasing. Compared with the United States and some European countries [1], practicing doctors per thousand persons in China are far less sufficient and their age distribution is also unbalanced, e. g., the younger practicing doctors are much more than the older, which poses new serious challenges to surgical training. Additionally, it is difficult to obtain real human tissues or organs for training, and they cannot be used repeatedly, which hinders quick and efficient training for young doctors. With the development of virtual reality technology, the emerging virtual surgery simulation can efficiently solve the above issues.

Virtual surgery simulation system is composed of a computer system and a force feedback system [2]. The displayer in the computer system can provide vivid display of surgery simulation for operators, and the force feedback system can provide accurate tactility, which allows virtual surgery experiments more accurate, realistic, reliable and efficient[3]. The modeling quality of virtual surgery determines the availability of the simulation system. Human soft tissues, such as esophagus, arm, trachea, thigh, intestine, appendix, gall bladder, stomach, and ureter may be twisted due to certain lesions or diseases [4]. Therefore, the study on the soft tissue torsion simulation is of great value and significance.

Generally, virtual soft tissue models can be divided into physical models and geometric models. Since the physical models consume too much time during the process of deformation, the geometric models are used much more widely in the soft tissue deformation due to fast real-time performance. For example, Zou, et al[5]. proposed a new meshless soft tissue deformation model based on point interpolation via a radial basis function, and set up a human liver model. The model can still perform better under the condition of complex topology changes, e. g., when performing cutting operation. Nevertheless, when the volume of soft tissue is relatively large, the real-time performance of the model will degrade. Camera, et al[6]. used location dynamic methods and realized nephrectomy simulation by constructing a surgery simulation platform with the help of a robot. However, when the area or volume of the deformed soft tissue becomes big, its elasticity will

① Supported by the National Natural Science Foundation of China (No. 61502240, 61502096, 61304205, 61773219) and the Natural Science Foundation of Jiangsu Province (No. BK20141002, BK20150634).
② To whom correspondence should be addressed. E-mail: zxr365@126.com
Received on Jan. 21, 2018

change with respect to iterations and constraint conditions of used algorithms, which will affect the accuracy of the model in deformation. Sack, et al[7]. used a non-mesh Galerkin method to realize the simulation of torsion and twisting deformation of virtual heart. Although the method can perform the modeling and simulation of heterogenous tissue, more experiments are needed to determine local model parameters, which will influence model practicality.

Based on biological nature of soft tissues in torsion, this work proposes a new coiling spring model with high accuracy, simple calculation and vivid interactive performance for meeting the requirements of the virtual surgery system in accuracy, speed and reliability.

## 1 Modeling of coiling spring model

As mentioned previously, surgical simulation requires that the used models have both realistic and real-time performances for soft tissue deformation. To this end, the proposed coiling spring model conducts soft tissue deformation via the superposition of torsional deformation generated on all circles in a coiling spring. When the proposed model is subjected to force, the forced process will show through three steps.

### 1.1 Rectangular coordinate system establishment

Assuming that the coiling spring model is placed at any point on the surface of the soft tissue, the rectangular coordinate system of the model is established as follows.

Under a given torque $M$, a coiling spring is set at any point $O$ on the soft tissue surface. Define $A_0$ as the outer point of rotatable core axis of the coiling spring, where the distance between point $O$ and $A_0$ is defined as $r$. The distance between $A_0$ and $O$ is $r$, which is defined as the radius of the rotatable core axis of the coiling spring. Define $O$ as the original point, and set up the $XYZ$ spatial coordinate system using the direction from point $O$ to $A_0$ as positive direction, as shown in Fig. 1.

Define the coiling spring according to every circle. The $i^{\text{th}}$ coil of coiling spring is a circle with radius $R_i$ that is centered at $O(0,0,0)$, radius $R_i$ is defined as

$$R_i = r + ih \tag{1}$$

where $h$ is the thickness of the $i^{\text{th}}$ coil of coiling spring, and $i = 1,2,3,\cdots\cdots,S$, and $S$ indicates the total coil number of used coiling springs. The width of cross section of the $i^{\text{th}}$ coil of coiling spring is $b$. The moment of inertia of the cross section is

$$I = \frac{bh^3}{12} \tag{2}$$

To determine the torque consumed by any coil of the coiling spring, the action line of the given torque $M$ is assumed to be tangent to the circle to which point $A_0$ belongs. Under a given torque $M$, if a total of $P$ coils of coiling spring produce torsional deformation in the soft tissue, then the $P^{\text{th}}$ coil of the coiling spring is defined as cutoff layer of torsional deformation, and $P \leqslant S$.

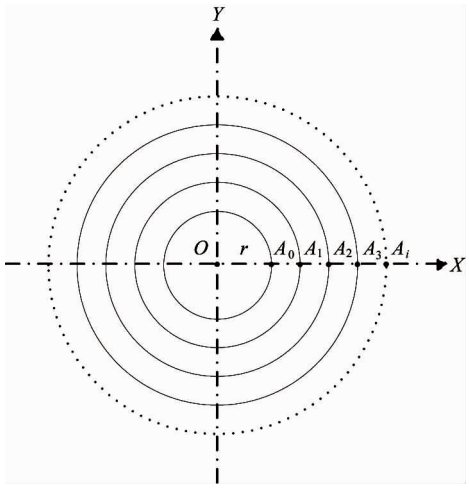


**Fig. 1** Cartesian coordinate system

### 1.2 Torque calculation of coiling springs

Assume that the maximum torsional force consumed by any point in the former $P-1$ coils of coiling springs under the action of the given torque $M$ equals $F_0$. Also, the maximum torsional force $F_P'$ consumed by any point in the $P^{\text{th}}$ coil of coiling spring under the action of the given torque $M$ is equal, and no more than $F_0$.

In the former $P-1$ coils of coiling springs, the total torque $M_i$ consumed by all points in the $i^{\text{th}}$ coil of coiling spring is

$$M_i = l_i \cdot F_0 = 2\pi R_i \cdot F_0 \tag{3}$$

where $l_i$ is the effective length of the $i^{\text{th}}$ coil of coiling spring, and $R_i$ is the radius of the $i^{\text{th}}$ coil of coiling spring. The total torque $M_P'$ consumed by all points in the $P^{\text{th}}$ coil of coiling spring is calculated by

$$M_P' = M - \sum_{i=1}^{P-1} M_i \tag{4}$$

Under the given torque $M$, the maximum torsional force $F_P'$ consumed by any point in the $P^{\text{th}}$ coil of coiling spring is

$$F_P' = \frac{M_P'}{2\pi R_P} = \frac{M_P'}{2\pi(r + Ph)} \tag{5}$$

### 1.3 Twisted coil number

The twisted coil number $n_i$ of torsion oils in the $i^{\text{th}}$ coiling spring under the action of torque $M_i$ is calculat-

ed in the following equation:

$$n_i = \begin{cases} \dfrac{1.25 M_i l_i}{2\pi EI} & i = 1,2,3,\cdots,P-1 \\ \dfrac{1.25 M'_P l_i}{2\pi EI} & i = P \end{cases} \quad (6)$$

where elastic modulus $E$ depends on biological characteristics of soft tissue, and $l_i$ is the effective length of the $i^{th}$ coil of coiling spring, as shown in the following equation:

$$l_i = \begin{cases} 2\pi R_i & i = 1,2,3,\cdots,P-1 \\ \dfrac{M'_P}{F_0} & i = P \end{cases} \quad (7)$$

## 2 Simulation experiment

### 2.1 Simulation pipeline

The simulation pipeline includes three stages: establishment of initial virtual scene, real-time computation and human-computer interaction. In the first stage, three-dimension (3D) models of virtual soft tissue and surgical instrument are established to virtualize the whole work environment. In the second stage, real-time collision detection is implemented[8,9]. When the collision between virtual surgical instrument and soft tissue is detected, corresponding deformation of soft tissue model will be carried out according to the magnitude of imposed torque. In the third stage, force feedback is calculated and transported to operators by haptic devices. After image rendering[10,11], the soft tissue deformation will be presented on the displayer, which provides visual feedback for operators. The flow chart of whole surgical simulation based on torsion deformation is shown in Fig. 2.

### 2.2 Experimental platform building

To verify the validity of the proposed model, a virtual simulation platform is established. The hardware configuration includes Intel i7 4.0GHz CPU, 8GB RAM, NVIDIA GeForce GTX 750Ti graphics card, liquid crystal display and PHANTOM OMNI force tactile device of Senable Technology Company. The software is composed of Windows 7, VC++ 2016 and OpenGL API. Calf and arm are selected as the simulation objects in this study, and the simulation environment is shown in Fig. 3.

## 3 Experimental results

Virtual 3D model of calf is set up based on the built simulation platform , which is twisted under the

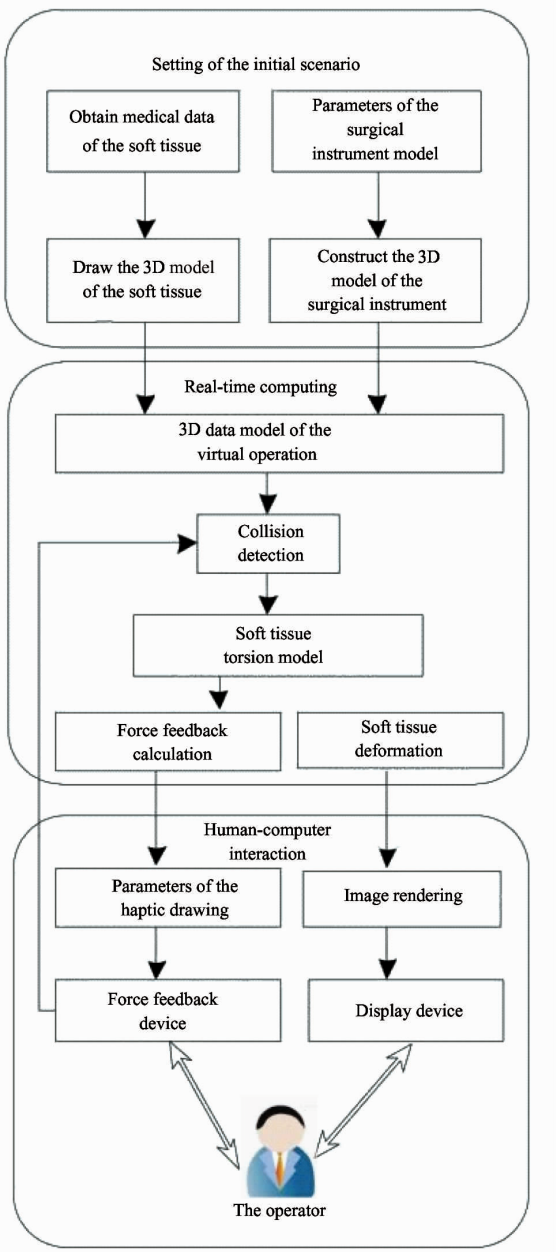


**Fig. 2** The flowchart of the model program

**Fig. 3** The simulation environment

action of given torque. In the experiments, shear modulus $G$ is set as $12.03 g/cm^2$, the imposed torque $M_T$ is set as $2.07 N \cdot m$, and the arm is simulated with 6185 particles and 12362 triangular meshes. Four sample images from three operational stages are selected to show the calf deformation process, as shown in Fig. 4. Seen from left to right in Fig. 4, the first image is the sampled image in initial stage, the second and third images are both from in-operation stage, and the fourth one is from the end stage of deformation simulation.

The torsion operation of arm is shown in Fig. 5, where four sampled images from four in-operation stages are selected. Seen from left to right in Fig. 5, the four images are captured at the beginning of the operation, the ending of the operation, one-third of the operation, and two-thirds of the operation, respectively.

During the operation, the virtual display of torsional deformation is smooth and clear, and the operator can detect continuous force feedback through the hand controller. The experimental results show that the visual and force feedbacks of arm torsion are better, which can meet the requirement of surgery simulation for real-time interaction.

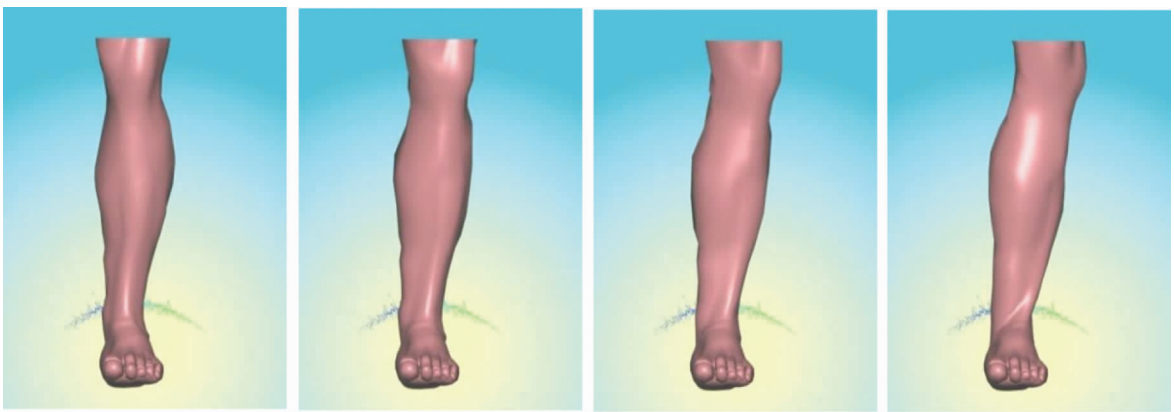

**Fig. 4** Torsion simulation of calf

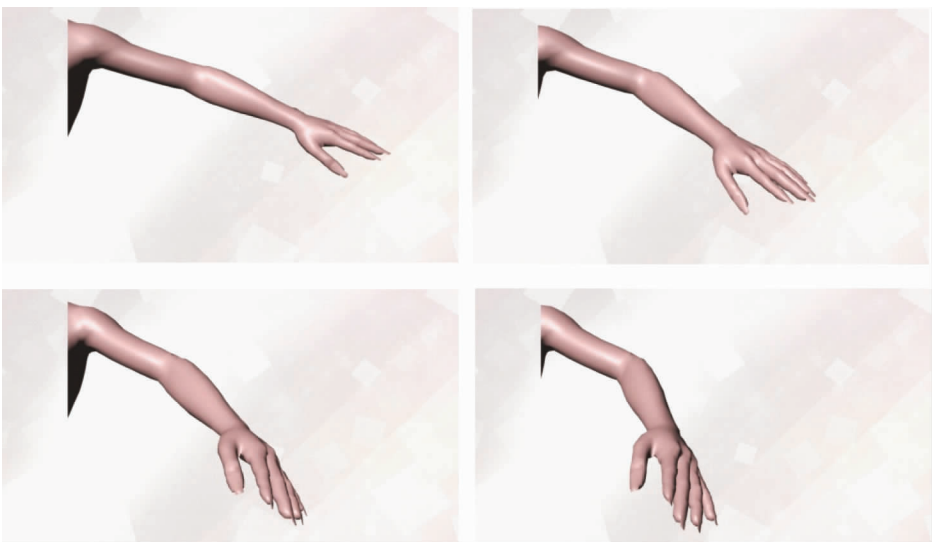

**Fig. 5** Torsion simulation of arm

## 4 Model analyses

### 4.1 Effect of torsion deformation

The visual feedback determines the accuracy of virtual surgery operation and overall simulation effect. Based on the same experiment platform, torsion operation based on the finite element model[12] is operated under the same torque and is shown in Fig. 6. Similar to the torsion operation shown in Fig. 5, four images in Fig. 6 are captured at the beginning, the ending, one-third and two-thirds of the operation, respectively. By comparing Fig. 5 and Fig. 6, the texture of the arm simulated by model is clearer, the visual effect is better, and the proposed model is superior to finite element model in image quality of torsion simulation.

**Fig. 6** Torsion simulation based on finite element model

## 4.2 Deformation time

Because of large amount of data calculation in the interactive operation for virtual surgical simulation, fast deformation is a basic requirement for virtual torsion operation. The real-time simulation system requires that the feedback time of surgery operation should be within the time range that human can perceive and respond to. Under the same experimental environment, same torque is applied to the arm torsion simulations based on the mass-spring model[13] (MSM), the finite element model (FEM), and the proposed model (PM). The deformation time after implementing virtual torsion operation is shown in Fig. 7. The experimental results show that the total deformation time of the proposed model is shorter than that of the finite element model and the mass-spring model, which indicates that model has better real-time performance.

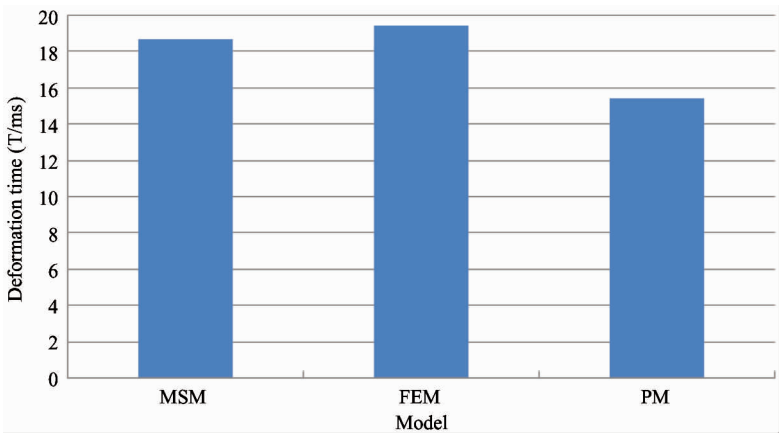


**Fig. 7** Deformation time

## 4.3 Deformation accuracy

In order to validate the accuracy of the proposed model, 3D Max software is used to construct a virtual arm model[14], where these parameters, such as the arm length, finger length and model thickness are set to be the same as that of real hand and arm under the same experiment environment[15]. Ten typical markers are selected on virtual arm model as well as real hand and arm, respectively, to record and express the displacement of every marker under the given same torque according to arm's characteristic in shape and torsion. The position of the ten typical markers on virtual arm model is the same as that on real hand and arm, which is shown in Fig. 8.

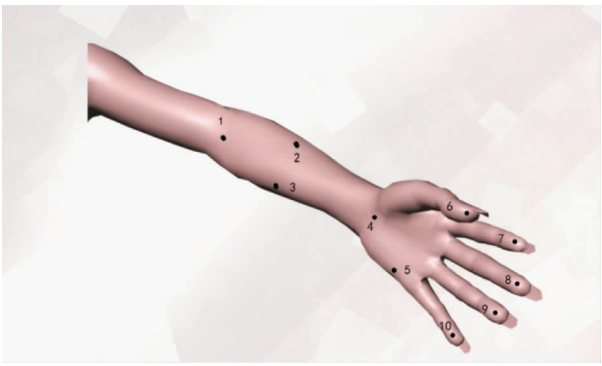


**Fig. 8** The position of ten typical markers

It is assumed that the initial coordinate of the ten typical markers on the virtual arm model in 3D coordinate system is defined as $O_i(x_0, y_0, z_0)$, and the coordinate after torsional operation is $O_i'(x_1, y_1, z_1)$. Displacement $H$ through torsional operation can be expressed as

$$H = \sqrt{(x_1 - x_0)^2 + (y_1 - y_0)^2 + (z_1 - z_0)^2} \tag{8}$$

The torsional displacements of the ten markers on the virtual arm model as well as real hand and arm are shown in Fig. 9.

To verify model accuracy during the torsional process, the 8th marker is selected as a sample point for investigating continuous deformation effect, whose displacement is recorded with time during the torsion operation. Torsional deformation is implemented under the same torque based on the mass-spring model, the finite element model, the real soft tissue and the proposed model, respectively, as shown in Fig. 10. The experimental results show that the difference between the displacement based on the proposed model and the displacement on real hand is the smallest, compared with other two models. Also, the proposed model can

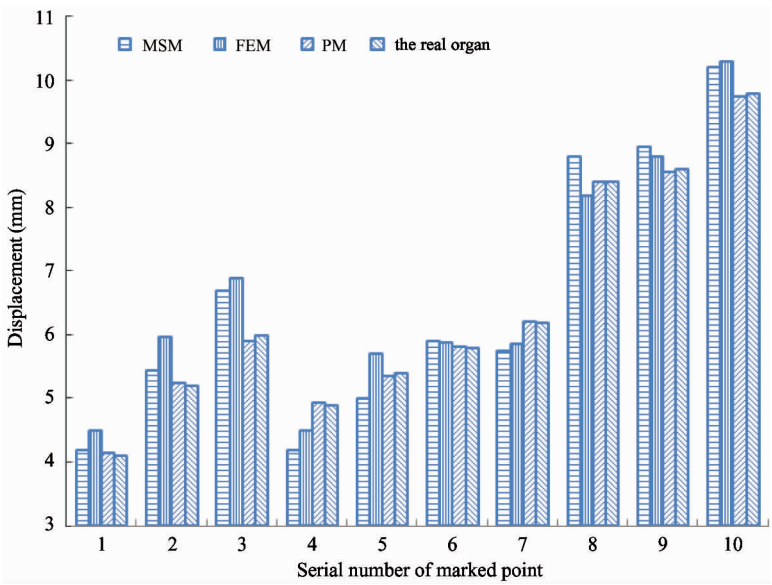


**Fig. 9** Displacement calculation on three virtual models and the real organ

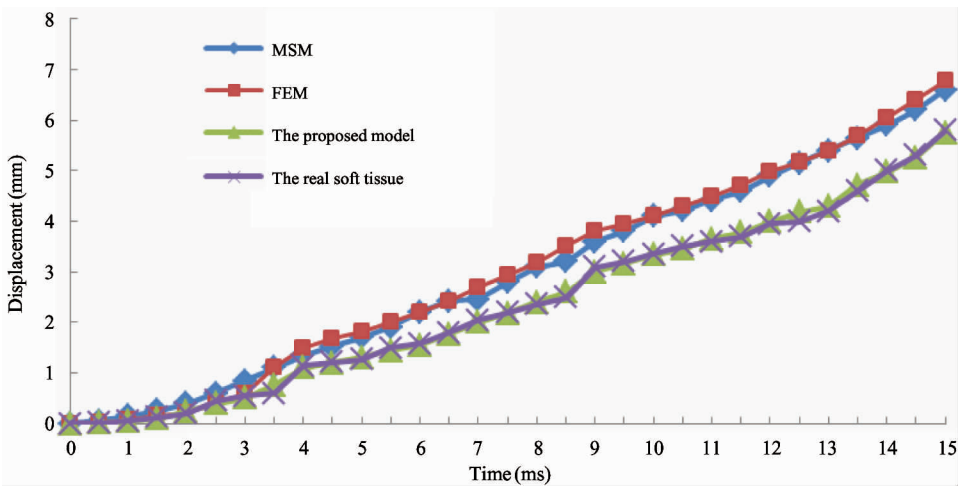


**Fig. 10** Displacements of the 8th marker during a continuous torsional process

achieve accurate torsion within short time when large deformation occurs, which indicates that the proposed model has high accuracy.

### 4.4 The evaluation of experimental effect

In order to verify the comprehensive performance of the proposed model, 40 physicians as subjects are randomly selected in the First Affiliated Hospital of Nanjing Medical University. Among them, there are 20 intern physicians, defined as $A_i$ (male 7, female 13), whose average age is 23, ten associate chief physicians, defined as $B_i$ (male 6, female 4), whose average age is 30, and 10 chief physicians, defined as $C_i$ (male 7, female 3), whose average age is 46. According to experience of inter physicians, associate chief physicians and chief physicians, three evaluation weights, i. e., 0.2, 0.3 and 0.5, are assigned to them, respectively. Nine evaluation indexes are designed to evaluate the proposed model. The 9 evaluation indexes include effectiveness, force feedback performance, real-time performance, system stability, deformation efficiency, fidelity, visual fluency, immersion, and texture features. The above indexes are numbered from 1 to 9 and their weights are 0.15, 0.15, 0.15, 0.15, 0.1, 0.1, 0.1, 0.05, and 0.05, respectively. The 40 subjects can conduct interactive operation through hand controller and the virtual arm, and then score the model from 0 to 10 points in terms of the above indexes.

The average score of each evaluation index is defined as $M$, which can be calculate by

$$M = 0.2 \cdot \left(\sum_{i=1}^{i-1} A_i/20\right) + 0.3 \cdot \left(\sum_{i=1}^{i-1} B_i/10\right) + 0.5 \cdot \left(\sum_{i=1}^{i-1} C_i/10\right) \quad (9)$$

where $A_i$, $B_i$ and $C_i$ are the $i^{\text{th}}$ evaluation index of the intern physicians, associate chief physicians, chief physicians respectively.

As is shown in Fig. 11, the lowest, the maximum, and the average scores of the proposed model are all higher than the mass-spring model and the finite element model. The experimental result shows that the proposed model has better performance.

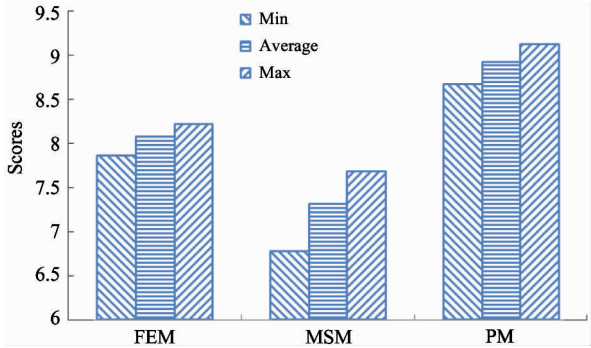


**Fig. 11** Model evaluation contrast

The variance $s_j^2$ of each evaluation index is defined as

$$s_j^2 = \frac{1}{A+B+C}\sum_{i=1}^{40}(x_i - M_j)^2 \quad (10)$$

where $x_i$ is the score evaluated by the $i^{\text{th}}$ physician for the proposed model, and $M_j$ is the average score of the $j^{\text{th}}$ evaluation index.

The comprehensive score of every evaluation index is given by

$$N = \sum_{i=1}^{4}(15\% \cdot M_i) + \sum_{i=5}^{7}(10\% \cdot M_i) + \sum_{i=8}^{9}(5\% \cdot M_i) \quad (11)$$

where $M_i$ is the average score of the $i^{\text{th}}$ evaluation index.

According to Eqs (9) and (10), the average score and variance of the three models are shown in Fig. 12 and Fig. 13, and the comprehensive score of the three models are shown in Fig. 14. Seen from the Fig. 13,

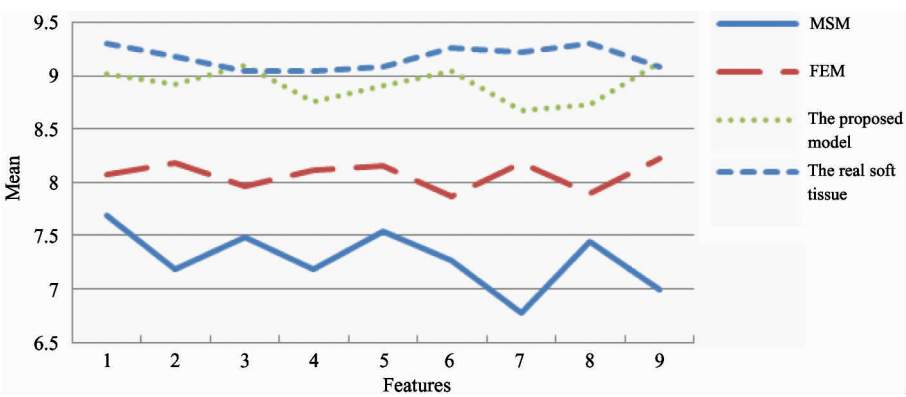


**Fig. 12** Average score contrast figure

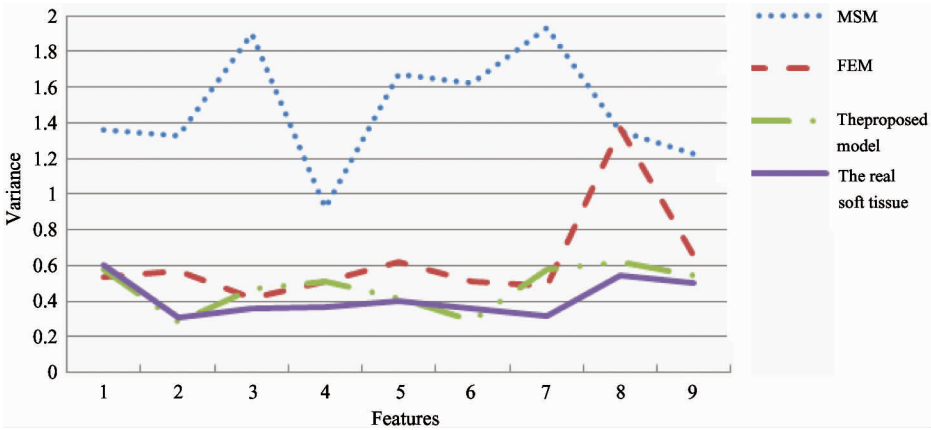


**Fig. 13** Variance contrast

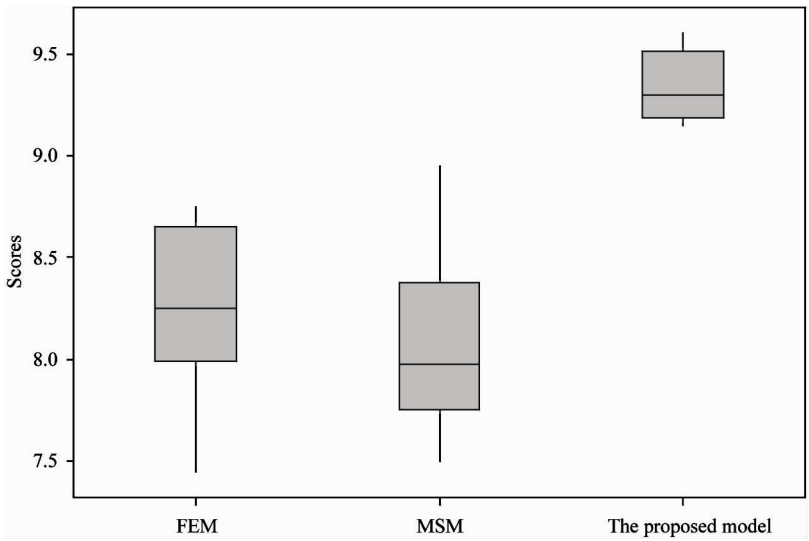


**Fig. 14** Comprehensive evaluation for models contrast

the variance of the proposed model is small, which indicates that the stability of the model is better. Therefore, the proposed model is validated to be better than other two state-of-the-art models.

### 4.5 Evaluation of training effect

In order to verify whether the constructed experimental platform based on the proposed model can help physicians to obtain experience of torsional operation as quickly as possible in the course of surgical treatment, 30 physicians (male 17, female 13) were invited randomly as subjects to implement torsional operation, whose average age is 24, and 10 chief surgical physicians (7 male, 3 female) were invited as evaluator to evaluate the operational effect on the experimental platform. The intern physicians and surgical chief physicians are all from the First Affiliated Hospital of Nanjing Medical University.

Before torsional operation experiment, the 30 intern physicians were averagely divided into three groups, i. e., every group includes 10 subjects. During torsional operation process, the first group physicians are allowed to spend 40min for training torsional operation on the proposed virtual arm model based on the proposed virtual experimental platform. The second group physicians are asked to firstly spend 20min for training by using the proposed virtual model on the virtual experimental platform, and then to spend 20min for training torsional operation on a real arm. The third group physicians are permitted to spend 40min for training same torsional operation on the real arm. The subjects in each group can take a rest of 5 – 10min during torsional operation process.

To verify the effect of the proposed model on improving subject's torsional operation ability, 10 chief surgical physicians were invited to score for the 30 subjects' torsional operation. The score is ranked from 0 to 10 points by the 10 chief surgical physicians according to subjects' performance in terms of operation proficiency and operation accuracy. The final score of ev-

ery intern physician is defined as the mean value of the scores from the 10 chief surgical physicians. Only 4 physicians were chosen to rest in the periods of 0 – 20min and 20 – 40min, and other physicians had no interruption during torsional operation. The evaluation results were recorded for the subjects at three different moments, respectively, to verify the efficiency of the proposed model in improving torsional operation ability. The torsional operation training can be divided into three stages based on the three moments. The moment before starting the torsional operation training is the first moment. The moment after training the subjects for 20min is the second, and the third moment is set after training the subjects for 40min.

The recorded results at the first moment for the subjects who are not trained are shown in Fig. 15. Without torsion operation experience, the scores of the three groups were generally lower and the difference between them is not large. Because the subjects are trained based on the virtual arm torsion model for 20min, the scores of the first group and the second group are a little higher than the third group. However, because the subjects are not trained based on real arm, the difference between the evaluated scores is small, as shown in Fig. 16. The evaluated results for the three groups at the third moment are shown in Fig. 17. The score of the subjects in the second group is obviously higher than that of the subjects in the other two groups, because the subjects in the second group experience two continuous and complete training both in the virtual and real arms. However, the score of the subjects in the first group is only a little higher than that of the subjects in the third group. The reason is that the subjects in the first group are trained for more time but not on the real arm. The variance of the evaluated score of three groups is shown in Fig. 18. Experimental results show that at the same time, the use of virtual torsional model can make surgical training more frequent. Also, the training in real arm after the training in virtual arm enables a better training effect, which implies that intern physicians can operate more proficiently and accurately in torsional operation if they are trained in the virtual arm based on the proposed model and then trained in real arm.

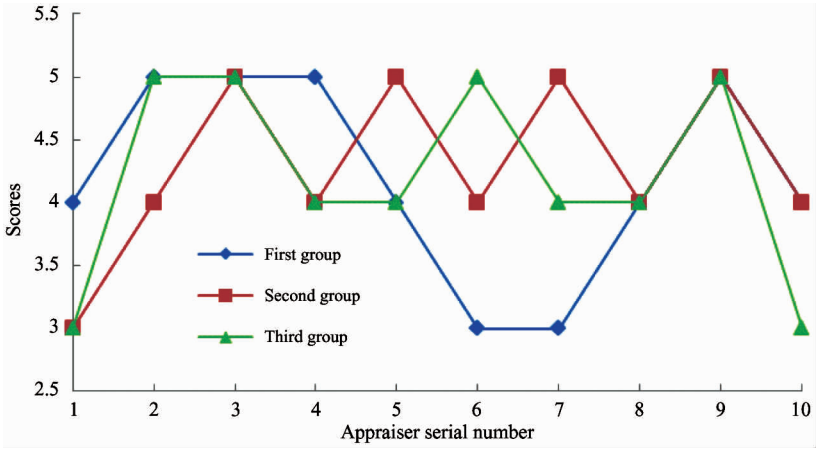


**Fig. 15** evaluation before training rendering

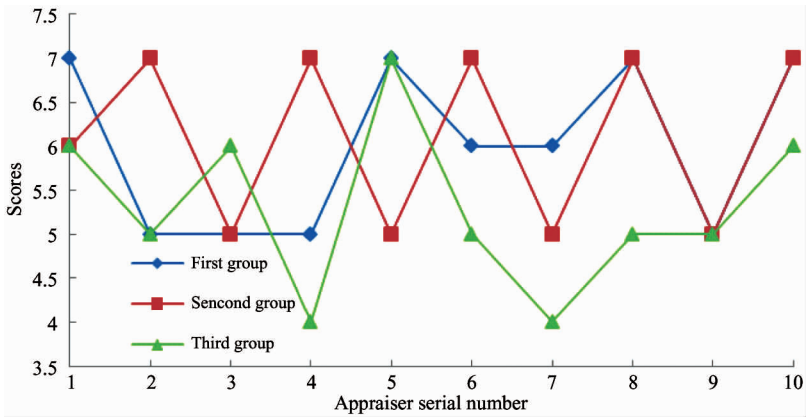


**Fig. 16** Midpoint of training time evaluation rendering

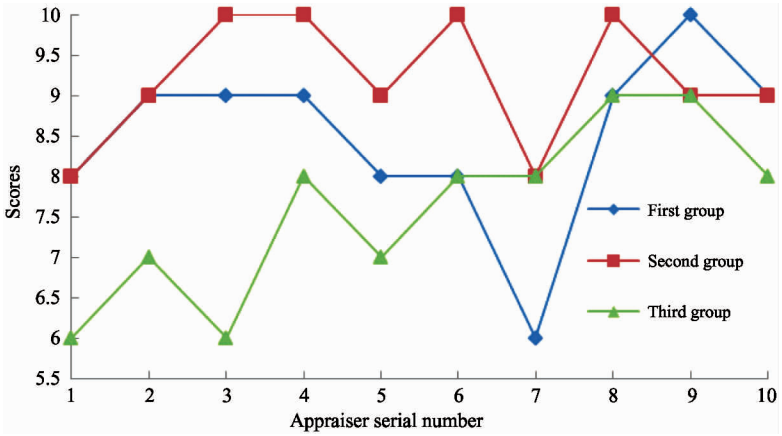


**Fig. 17** evaluation after training rendering

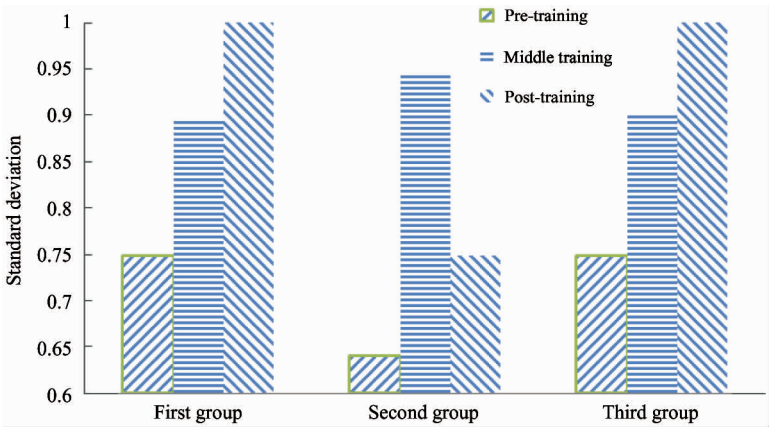


**Fig. 18** training evaluation standard

## 5 Conclusions

This paper proposes a coiling spring model for modeling torsional deformation of soft tissue. Haptic interaction devices are utilized in virtual simulation platform to realize the torsion deformation of human legs and arms. Compared with previous state-of-the-art models, the proposed model has better experience of torsional operation training. The experimental results show that the proposed model has competitive advantages in terms of real-time performance, interactive ability, model accuracy, and realistic quality.

There are still some limitations to be improved in this study. For example, the algorithm complexity will increase under large torsional deformation, and the graphics refresh rate will decrease. In future work, relative surgical knowledge and instructions of surgical operation can be imported to the virtual surgical training system, which will improve the training effect of surgical physicians in surgical operation.

**References**

[1] Puustjärvi J, Puustjärvi L. Towards web-assisted self-care in developing countries: a challenge for health posts and pharmacies[C]. In: Proceedings of IST-Africa Week Conference, Durban, South Africa, 2016. 1-10

[2] Wang D X, Jiao J, Zhang Y R, et al. Computer haptics: haptic modeling and rendering in virtual reality environments[J]. *Journal of Computer-Aided Design & Computer Graphics*, 2016, 28(6): 881-895

[3] Shao X Q, Nie X, Wang B Y. GPU-based real-time 3D visual hull reconstruction and virtual-reality interaction [J]. *Journal of Computer-Aided Design & Computer Graphics*, 2017, 29(1): 52-61

[4] Freutel M, Schmidt H, Dürselen L, et al. Finite element modeling of soft tissues: material models, tissue interaction and challenges[J]. *Clinical Biomechanics*, 2014, 29(4): 363-372

[5] Zou Y, Liu P X, Cheng Q, et al. A new deformation model of biological tissue for surgery simulation [J]. *IEEE Transactions on Cybernetics*, 2016, 47(11): 3494-3503

[6] Kim Y, Kim L, Lee D, et al. Deformable mesh simulation for virtual laparoscopic cholecystectomy training[J]. *Visual Computer*, 2015, 31(4): 485-495

[7] Sack K L, Skatulla S, Sansour C. Biological tissue mechanics with fibres modelled as one-dimensional Cosserat continua, applications to cardiac tissue[J]. *International Journal of Solids and Structures*, 2016, 81: 84-94

[8] Goulette F, Chen Z W. Fast computation of soft tissue defor-mations in real-time simulation with Hyper-Elastic Mass Links[J]. *Computer Methods in Applied Mechanics and Engineering*, 2015, 295: 18-38

[9] Zou Y, Liu P X, Yang C, et al. Collision detection for virtual environment using particle swarm optimization with adaptive cauchy mutation[J]. *Cluster Computing*, 2017, 20(2): 1765-1774

[10] Suaib N M, Nasir F M. Broad phase collision detection using graphics processing unit[J]. *International Journal of Innovative Computing*, 2016

[11] Kao C C. Stereoscopic image generation with depth image based rendering[J]. *Multimedia Tools and Applications*, 2017, 76(11): 12981-12999

[12] Yang L, An P, Liu D, et al. 3D holoscopic images coding scheme based on viewpoint image rendering[C]. In: International Forum of Digital TV and Wireless Multimedia Communication, Shanghai, China, 2016. 318-327

[13] Ganganagoudar A, Mondal T G, Prakash S S. Analytical and finite element studies on behavior of FRP strengthened RC beams under torsion[J]. *Composite Structures*, 2016, 153: 876-885

[14] Zhang X R, Zhu J D, Sun W, et al. Virtual brain surgery simulation system based on haptic interaction[J]. *High Technology Letters*, 2015, 21(2): 185-191

[15] Qiao G, Gao H, Cheng P, et al. Ground demonstration system based on in-orbit assembly oriented manipulator flexible force control[J]. *High Technology Letters*, 2017, 23(3):271-278

**Zhang Xiaorui**, born in 1979. She received her Ph. D degrees in Instrument Science and Technology Department of Southeast University in 2010. She also received her B. S. and M. S. degrees from Henan University of Science and Technology in 2004 and 2007 respectively. Her research interests include the virtual reality, human-computer interaction, and image processing.